Open access • Proceedings Article • DOI:10.23919/EUCAP.2017.7928667

Coupled dipole antennas for on/off-body communications at 2.45 GHz

Haoran Su, Robert M. Edwards, Elijah I. Adegoke

Institutions: Loughborough University

Published on: 01 Jan 2017 - European Conference on Antennas and Propagation

Topics: Dipole and Dipole antenna

Coupled Dipole Antennas for On/Off-Body Communications at 2.45 GHz

Haoran Su*, R. M. Edwards*, Elijah I. Adegoke*
*The Wolfson School. Mechanical, Electrical and Manufacturing Engineering
Loughborough University, Loughborough, UK
Email: r.m.edwards@lboro.ac.uk

***Abstract*—In this paper, three experiments with coupled dipoles were carried out in order to determine the optimal distance where an efficient communication link can be established. The simulations results showed that when the subcutaneous dipole is installed adjacently to the surface of the skin, the dipole mounted above the skin level should be in the range of 20 mm to 25 mm for efficient communication. Subsequently, the influence of the dielectric parameters of the human tissue on wave propagation has also been presented in this work.**

***Keywords*—on-body antennas; Medical Implants; Body area networks; body-centric wireless communications; on-body propagation.**

I. Introduction

With the development of mobile communications technology, body centric wireless devices are becoming a topical field for contemporary research. In particular, the escalating demand for effective and efficient communications for these devices has resulted in the development of wearable textiles systems. Body centric wireless communications occur within a small range of personal area networks (PAN) and body area networks (BAN) [1]. Wearable textile systems basically consist of textiles and electronics aimed at improving the experience of the wearers. Recent research shows that typical applications of the wearable textile systems are wearable radio frequency identifications (RFIDs) and smart fabrics and interactive textiles (SFIT) [2]. The development of new conductive materials allows wearable RFIDs and SFIT to be unobtrusively integrated on smart garments. The new generation of garments will provide the functionality of monitoring the conditions of the wearers health and the environment [3]. Concurrently, the data acquired by these devices needs to be transmitted to a care giver (via a base-station) for pre diagnosis or for patient condition monitoring. This makes the antennas involved in the communication channel critical to achieving effective communication between the wearable textile system and a base-station.

Typical smart garments adopt a wired feeding technique (such as coax feed) to connect he antenna to the transceiver. However, this usually limits the wearer's movement and degrades performance in practical applications. New techniques such as magnetic coupling [4] can be used as an alternative. This method utilizes the transformer structure to connect the feed with the antenna, thus eliminating galvanic contacts between the feed and the antenna. Magnetic coupling feeding is realized by implementing two coils of the transformer on the antenna and the RFID chip respectively. As a result, the RFID chip can be mounted on the flexible substrate either by placing or gluing [4]. In most cases, communication channels for medical implants require that physical cables are attached to patients for data transfer, this however limits the patient's mobility. This restriction can be limited by using on body antennas attached to human skin [5]. In general, there are five known ways of establishing a communication link between medical implants and on-body antennas. They are : Electromagnetic induction, MICS band, ISM band, acoustic links and optical cables. Electromagnetic induction examples include pacemakers, which require a coil to be placed on the chest of patients during medical examination. In this case, the inductively coupled coils in the two devices can set up the communication link. However, the low data rate and bandwidth limits the communication since it is operating at a low frequency [6]. The medical implant communication service (MICS) can be utilized for communications between base-stations and medical implants or communications between medical implants within the same body. According to the ETSI, the spectrum from 402 MHz to 405 MHz has been set aside for the applications of MICS [7]. The maximum bandwidth for each channel is 300 kHz, which means that MICS can accommodate ten channels at most. In addition, the maximum transmitting power for MICS is 25 μW EIRP. The 2.45 GHz industrial, scientific and medical (ISM) radio band can also be used with maximum EIRP of 100 mW [7]. The frequency band used is from 2.4 GHz to 2.5 GHz. The systems using this band often make use of frequency hopping spread spectrum (FHSS) or direct sequence spread spectrum (DSSS) to share radio resources. Acoustic links could also be used for establishing communication links between medical implants and on-body antennas [8]. This requires an embedded converter in the bio-sensor that can convert the external acoustic signal to power the sensor. The sensor then uses the acoustic signal to transmit the data to the receiving equipment outside the body. Optical links can also be adopted in certain situations where the medical implants is placed close to the skin surface. In this paper, the influence of the dielectric properties of the human tissue on wave propagation and determining the optimal distance for on-body antennas will be discussed.

Table I
DIELECTRIC PARAMETERS OF HUMAN TISSUE AT 2.45 GHZ [10]

Human tissue	ϵ_r	σ (S/m)
Skin (dry)	38	1.46
Skin (wet)	42.85	1.59
Fat	54.42	1.88
Blood	5.28	0.10
Bone (cancellous)	18.55	0.81
Gray matter	48.91	1.81
White matter	36.17	1.21
Lung (inflated)	20.48	0.80
Lung (deflated)	48.38	1.68
Heart	54.81	2.26
Kidney	52.74	2.43
Stomach	62.16	2.21
Eyes	52.63	2.03

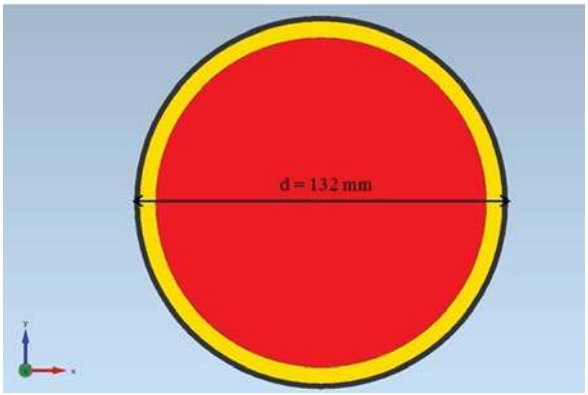

Figure 1. Cross-section of male upper arm

II. ELECTRICAL PROPERTIES OF THE HUMAN TISSUE

There are two popular data sets available for the dielectric properties of the human tissue. One is the Debye model which is used to simulate the dielectric parameters of the human tissue for the measurement in a physical phantom [9] and the other is given by Gabriel, which is used for measurement on the human body [10]. The latter should be used for analyzing the performance of implanted antennas. In Table I, the relative permittivity (ϵ_r) and conductivity (σ) of different human tissues are presented. These values are highly influential in the performance of implanted antennas. Body tissue simulating liquids are widely used for measurements relating to implanted antenna as well and specific absorption rate (SAR) of mobile handsets. The tissue simulating liquids usually consist of six different ingredients which are: water, sugar, salt (NaCl), cellulose, preservatives and DGMBE. Water is used as core ingredient for the body tissue simulating liquid. DGMBE is a chemical used to reduce relative permittivity of the liquid. Salt is used to increase the conductivity. The presence of cellulose helps increase viscosity and ensures that the sugar is kept in the solution. Preservatives are used to prevent the spread of bacteria and molds.

Usually, the performance of an antenna is affected when it is attached to an object. This phenomenon is likely to hold when an antenna is attached to or inserted into a human body. For implanted antennas, the antenna is surrounded by human tissue in all directions. Therefore, the influence produced by the human tissue needs to be taken into account when studying the performance of an implanted antenna. In [5], a detailed study of the wave propagation attenuation is presented with respect to the electric and magnetic fields.

III. SIMULATING DIPOLES IN FREE SPACE AND MATTER

Empire version 7.0 was used for the simulation carried out in this section. Default settings have been adopted with the dielectrics changed to *medium band lossy* and the conductors set to be *lossless*. The simulation uses an adult male upper arm as a research object to investigate the performance of both single dipole and coupled dipoles near the human tissue. Based on [11], the human upper arm could be simplified as a cylinder. The average length of adult male upper arm is 42.9 cm and its circumference is 41.7 cm. In the simulation, the upper arm model has been simplified to three layers(see Figure 1), which include : skin (black layer), fat (yellow layer) and muscle (red layer). The average thickness of the skin is 2 mm in the upper arm and the thickness of fat is 5.5 mm. The rest of the arm can be regarded as being filled with muscle with radius is 58.5 mm [11].

In Figure 2, the layout of the simulation is presented. The The dipole antenna inside the skin is encapsulated in the glass box because the metallic arms of dipole can be harmful to human tissue (It should be noted that SAR results are not included in this work). It is placed parallel to the central axis of the cylinder underneath the skin. The center of the dipole is at the same level as the geometric center of the cylinder. The second dipole is located above the skin parallel to the dipole inside the skin (whose center is also at the same level as the geometric center of the cylinder). The wavelength can be decreased in the tissue due to the increase in the relative permittivity of the tissue [12]. The length of the dipole was shortened in order to make the dipole in the skin work at 2.45 GHz. The length and diameter of the dipole in the skin is 24.8 mm and 4.9 mm(see Figure 3). The glass box is a cuboid with a squared bottom whose side is 5.9 mm long and the height of the glass box is 25.8 mm. The relative permittivity of the glass box is 4.8. The dipole inside the glass box is 0.5 mm away from each surface of the box (see Figure 4). The dipole outside the body is a half-wavelength dipole with length 61.2 mm at the frequency of 2.45GHz. However, in order to improve the match of the dipole, the length of the dipole was shortened to 0.43λ.

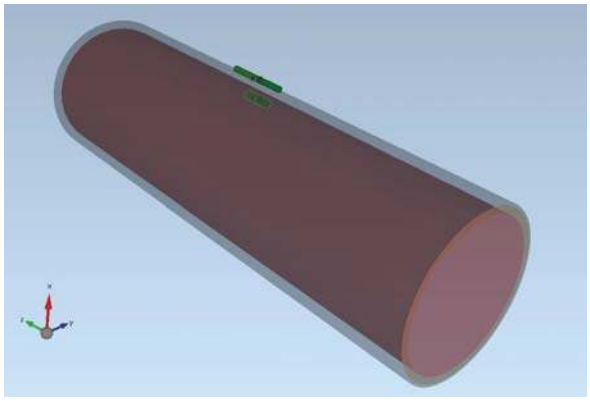

Figure 2. Layout of the simulation of two coupled dipoles

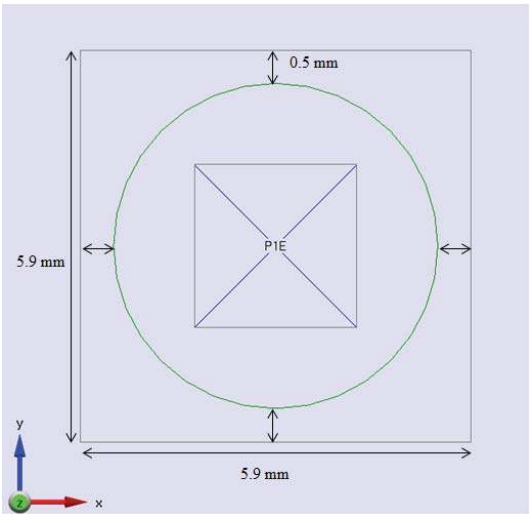

Figure 4. Top view of dipole encapsulated in the glass box

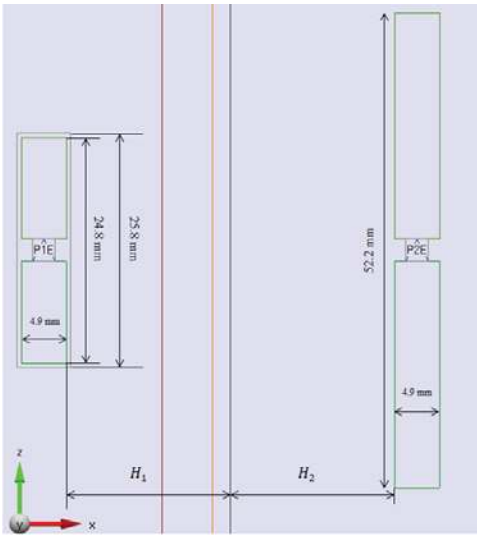

Figure 3. 2D front view of two coupled dipoles

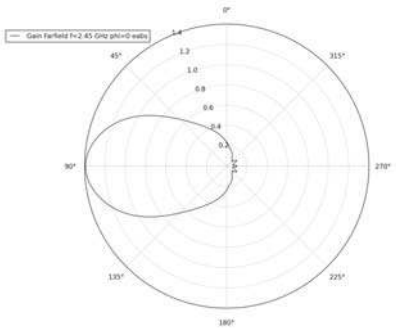

Figure 5. Polar plot of dipole above the heterogeneous arm model at 2.45 GHz

A. *Performance of single dipole near human tissue*

In order to investigate the influence of human tissue on the performance of a single dipole, the simulation with one dipole above the arm model has been conducted and the results of simulation will be presented in this section. The dimension of dipole simulated is the same as above. It was observed during that the S_{11} varies between with the distance between the dipole and the arm. The separating distance was varied from 1 mm to 30 mm and the lowest S_{11} (of -29.47 dB at 2.44 GHz) was observed at 13.1 mm (0.11λ). This value however shows a 21.4% deviation from the theoretical value of 0.14λ. In order to reduce the deviation between the simulation and theoretical value, the relative permittivity and conductivity of the human tissue were adjusted to average values of 32.6 and 1.15 S/m. Using these parameters, a minimum S_{11} (of -53.57 dB at 2.32 GHz) was observed at 15.7 mm (0.13λ). The maximum gain of the dipole was 2.86 dBi at 2.45 GHz and the simulated E-field is shown in Figure 5. The input impedance of the dipole was 53.72 + j0.73 Ohms.

B. *Performance of coupled dipole near human tissue*

The impact of the human tissue and determining the optimal separating distance for the coupled dipoles is presented in this section. Three simulation scenarios were carried out and are discussed. The antenna pair layout for the three scenarios is the same as Figure 2.

1) Simulation scenario 1: The subcutaneous dipole was fixed at the distance of 1 mm (H_1) away from the surface of skin. The dipole above the skin was gradually moved further away from the skin in order to investigate the influence of the separating distance. The separating range used was from 0 mm to 30 mm (λ/4), at (λ/4), the coupling effect between two dipoles becomes negligible [13]. The lowest S_{11} (of -15.50 dB at 2.45 GHz) was observed at 23.5 mm (H_2) and the corresponding S_{21} was -17.76 dB. The input impedance of the dipole above the skin was 36.74 + j6.10 Ohms.

2) Simulation scenario 2: The antenna above the skin was fixed at the distance of 2 mm to the surface of skin (H_2) and the subcutaneous dipole was varied like in Scenario 1 in order to determine the point where the optimal S_{11} and S_{21} occurred. The lowest S_{11} (of -14.46 dB at 2.45 GHz) was observed at 5.25 mm (H_1) and the corresponding S_{21} was -13.68 dB. The input impedance of the subcutaneous dipole at this location was 34.27 + j2.64 Ohms. This implies less energy was stored in the near field in spite of the notable impedance mismatch.

3) Simulation scenario 3: The initial position of both antennas were 1 mm away from the surface of the skin. Both dipoles were then moved equal distances away from the skin. The optimal S_{11} and S_{21} observed were -14.37 dB and -13.38 dB at 5.1 mm ($H_1 = H_2$). The input impedance of the subcutaneous dipole at this location was 34.07 + j2.31 Ohms. The match has been slightly improved compared with simulation 2, since the subcutaneous dipole is more adjacent to the surface of the skin.

IV. Analysis of simulation results

A. Single dipole case

From the simulation results above, it is apparent that an optimal location exists, where the S_{11} of the dipole can reach the minimum. For the heterogeneous arm model simulation, the variation of S_{11} in terms of distance away from the skin is shown in Figure 6. The Figure indicates that the S_{11} moves to a lower frequency with increasing separating distance between the dipole and the skin (except for D = 1 mm). When the dipole is placed 1 mm away from the surface of skin, S_{11} was detuned to a lower frequency. This is because the reflection from the skin becomes dominant. The bandwidth of the antenna also decreases to the minimum before the optimal point. However, it expands after the optimal point with the antenna moved further away from the skin. The magnitude of the S_{11} also follows the same variation pattern as the bandwidth. As for the homogeneous arm model (with adjusted parameters), the variation pattern of the S_{11} is similar to the heterogeneous arm model. However, the S_{11} reaches -53.56 dB at the optimal point (see Figure 7). The simulated efficiency for both arm models also increases with the distance between the dipole and the skin. Nonetheless, the homogeneous model gives better results.

B. Coupled dipole case

For the first coupled dipole scenario, the resonant frequency decreased with increased separation distance. This variation

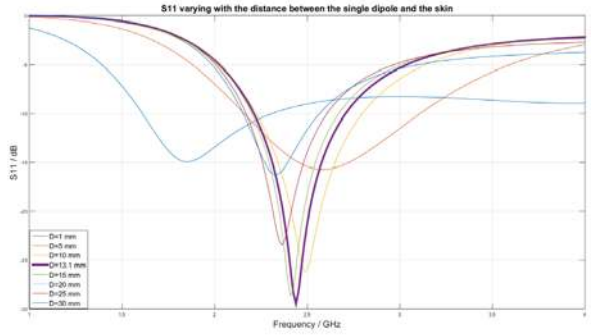

Figure 6. S_{11} with heterogeneous arm model and varying distance

also applied to the S_{21} which indicates that the power transmitted from the subcutaneous antenna to the antenna outside has been declined due to the increase of the distance between the two dipoles. However, the increase in the S_{11} suggests more power gets reflected (see Figure 8). For the second scenario, the S_{11} variation is shown in Figure 9. It is evident that the S_{11} moves to a lower frequency and the bandwidth expands with increasing separation distance. However, the resonant frequency was detuned to 1.99 GHz at the distance of 10 mm which is as a result of reflection from the boundary between the muscle and the fat. The boundary was situated 7.5 mm away from the surface of skin and would vary from individuals. In the final scenario, the S_{11} is shown in Figure 10. It can be seen that the variation is identical to Scenario 2, which suggests that the resonant frequency drops before and after the boundary between the muscle and fat. In addition, the reflection at the boundary becomes a major factor influencing the resonant frequency within boundary regions. While the antennas can operate at both distances of 5.1 mm and 12.5 mm, the distance of 5.1 mm has been selected, since less power is reflected and more power transmitted to the antenna outside the skin.

As far as the performance of coupled dipoles is concerned, the S_{21} decreases consistently as the distance between the dipoles increases. This is probably due to the reduction of coupling effect between two dipoles. Therefore, it becomes necessary to compromise between the S_{11} and the S_{21} in determining the distance where the optimal S_{11} and S_{21} can be attained.

V. Conclusion

This work has been able to show that the operating frequency, skin boundaries and tissue properties can affect the magnitude of the attenuation experienced by a propagating wave. Optimal separation distances have been determined for single and coupled dipoles for on-body antenna communication systems. The outcome of the second scenario for coupled dipoles presents an advantage for medical implants. This can

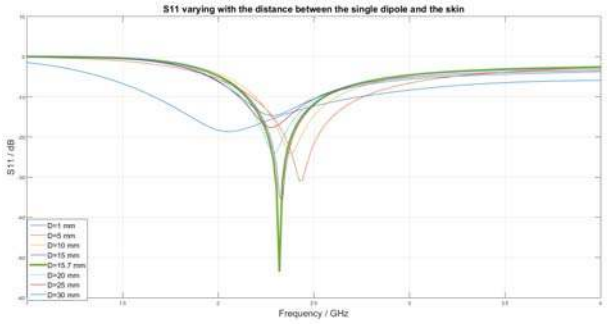

Figure 7. S_{11} with homogeneous arm model and varying distance

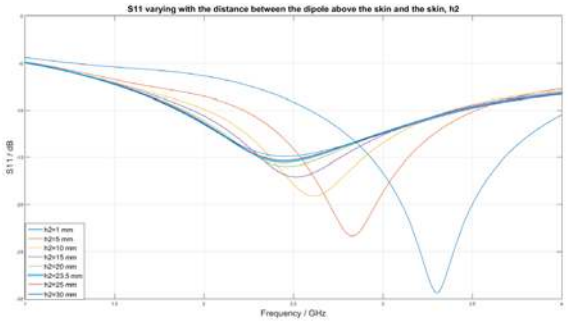

Figure 8. Variation of S_{11} with separation distance between the dipole and the skin

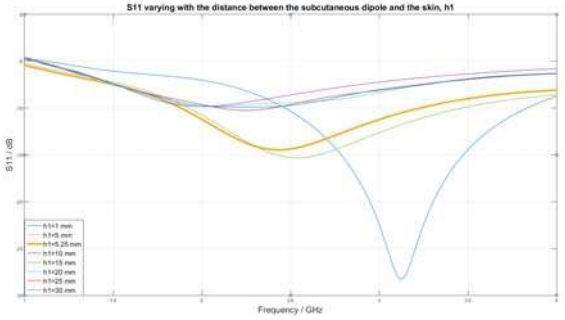

Figure 9. Variation of S_{11} with separation distance between the subcutaneous dipole and the skin

simplify the installation process and reduce the operation difficulty while still maintaining maximum power transfer for shallow depth medical implants.

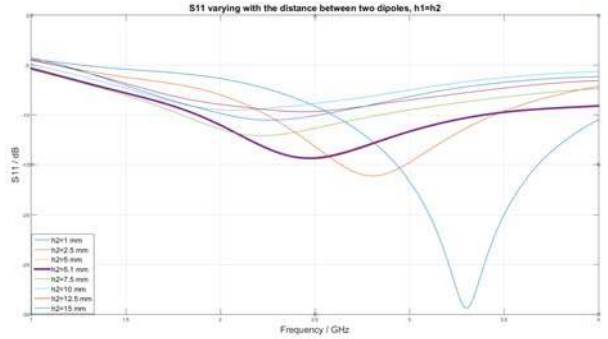

Figure 10. Variation of S_{11} with equal separation distance between the dipoles

REFERENCES

[1] P. S. Hall and Y. Hao, "Antennas and propagation for body centric communications," in *2006 First European Conference on Antennas and Propagation*, Nov 2006, pp. 1–7.

[2] M. Virili, H. Rogier, F. Alimenti, P. Mezzanotte, and L. Roselli, "Wearable textile antenna magnetically coupled to flexible active electronic circuits," *IEEE Antennas and Wireless Propagation Letters*, vol. 13, pp. 209–212, 2014.

[3] C. Hertleer, A. Tronquo, H. Rogier, L. Vallozzi, and L. V. Langenhove, "Aperture-coupled patch antenna for integration into wearable textile systems," *IEEE Antennas and Wireless Propagation Letters*, vol. 6, pp. 392–395, 2007.

[4] F. Alimenti, M. Virili, G. Orecchini, P. Mezzanotte, V. Palazzari, M. M. Tentzeris, and L. Roselli, "A new contactless assembly method for paper substrate antennas and uhf rfid chips," *IEEE Transactions on Microwave Theory and Techniques*, vol. 59, no. 3, pp. 627–637, March 2011.

[5] A. J. Johansson, "Wireless communication with medical implants: Antennas and propagation," Ph.D. dissertation, Lund University, 2004.

[6] J. Webster, I. E. in Medicine, and B. Society, *Design of Cardiac Pacemakers*, ser. Studies in Asian Thought and Religion. IEEE, 1995. [Online]. Available: https://books.google.co.uk/books?id=W1VyQgAACAAJ

[7] ETSI, "ETSI EN 301 839 V2.1.1 ETSI." [Online]. Available: http://www.etsi.org

[8] E. Doron and A. Penner, "Acoustic biosensor for monitoring physiological conditions in a body implantation site," Nov. 26 2002, uS Patent 6,486,588. [Online]. Available: https://www.google.si/patents/US6486588

[9] A. Sihvola and I. of Electrical Engineers, *Electromagnetic Mixing Formulas and Applications*, ser. Electromagnetics and Radar Series. Institution of Electrical Engineers, 1999. [Online]. Available: https://books.google.co.uk/books?id=uIHSNwxBxjgC

[10] C. Gabriel, "Compilation of the Dielectric Properties of Body Tissues at RF and Microwave Frequencies," 1996. [Online]. Available: www.dtic.mil/dtic/tr/fulltext/u2/a305826.pdf

[11] National Health Statistics, "Anthropometric reference data for children and adults: United States, 20032006." National health statistics reports," 2008. [Online]. Available: www.cdc.gov/nchs/data/series/sr_03/sr03_039.pdf

[12] R. King and G. Smith, *Antennas in matter : fundamentals, theory and applications*. MIT Press, 1981. [Online]. Available: https://books.google.co.uk/books?id=19FDnwEACAAJ

[13] J. H. Kim, S. I. Cho, H. J. Kim, J. W. Choi, J. E. Jang, and J. P. Choi, "Exploiting the mutual coupling effect on dipole antennas for rf energy harvesting," *IEEE Antennas and Wireless Propagation Letters*, vol. 15, pp. 1301–1304, 2016.